Contraction and Collapsing Kinetics of Single Synthetic Polymer Chains at Small Quench Depths

Jinming Hu, Di Wang, Jian Xu, Zhiyuan Zhu, Shiyong Liu*

Chain contraction and collapsing kinetics of pyrene-labeled poly(*N*-isopropylacrylamide) (PNIPAM) single chains ($\overline{M}_n = 3.64 \times 10^5$ g · mol^{-1}, $\overline{M}_w/\overline{M}_n = 1.17$) were investigated by employing the stopped-flow technique coupled with fluorescence and light scattering detections, which can achieve millisecond jumping of solvent quality from good to above and below the θ-solvent condition at small quench depths. It was found that the coil-to-crumpled globule transition proceeds via an isotropic one stage process and the obtained characteristic relaxation times exhibit a monotonic decrease with increasing quench depths. The obtained experimental results were in qualitative agreement with previous theoretical considerations.

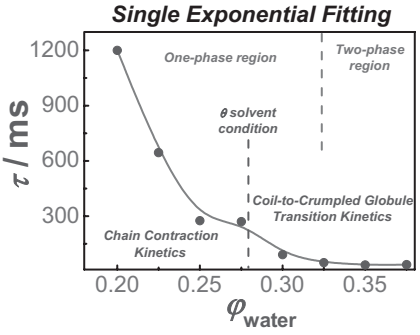

Introduction

In good solvents, polymer chains adopt an extended coil conformation due to repulsive segment-segment interactions. At the θ-solvent conditions, the chains exhibit nearly unperturbed dimensions because chain segment-segment interactions just balance the chain segment-solvent interactions. In a very poor solvent, the dominance of attractive segment-segment over segment-solvent interactions will force the polymer chain to collapse into the globular states.[1,2] Due to its partial resemblance to protein and DNA folding,[3–5] the conformational transition of long polymer chains from the extended coil state to compact globules (coil-to-globule transition) has been the subject of extensive studies in the past few decades,[6–21] which mainly focused on the thermodynamics of the coil-to-globule transition, i.e., the evolution of equilibrium chain conformations as the solvent quality slowly varies to span across the θ-solvent condition.

Among previously investigated systems, poly(*N*-isopropylacrylamide) (PNIPAM) has been frequently chosen, which possesses a coil-to-globule transition near the lower critical solution temperature (LCST) at ≈32 °C.[12] Using laser light scattering, Wu et al.[13,17,22] were able to detect thermodynamically stable globules in the absence of any aggregates, but only within a relatively narrow temperature range. Halperin et al.[23] employed Monte Carlo simulation to investigate annealed copolymers of solvophobic/solvophilic monomers and explained the presence of stable PNIPAM globules. On the other hand, PNIPAM also exhibits the so-called "co-non-solvency" phenomenon. It can unimolecularly dissolve in water and methanol, respectively, but not in a proper mixture of them.[24–26] The equilibrium structures of single PNIPAM chains ($\overline{M}_w = 2.6 \times 10^7$ g · mol^{-1}) in extremely dilute solution as a function of methanol/water compositions have been investigated by Wu et al.,[27] revealing a re-entrant coil-to-globule-to-coil transition behavior. In pure methanol, PNIPAM chains exist as extended coils; in the volume fraction of water (φ_{water}) range of 0.3 – 0.4, PNIPAM chains partially collapse into crumpled globules; in the φ_{water}

J. Hu, D. Wang, J. Xu, Z. Zhu, S. Liu
CAS Key Laboratory of Soft Matter Chemistry, Department of Polymer Science and Engineering, Hefei National Laboratory for Physical Sciences at the Microscale, University of Science and Technology of China, Hefei, Anhui 230026, China
E-mail: sliu@ustc.edu.cn

DOI: 10.1002/macp.201000476

range of 0.4 – 0.7, PNIPAM chains remain in the compact globule state; further addition of water leads to the re-swelling of globules into random coils.

It has been proposed that, in certain cases, protein folding proceeds first via a fast non-specific hydrophobic collapse to a molten globule state, after which native contacts are established via a slower process as the protein approaches its native structure. Thus, fully understanding the collapsing kinetics of synthetic polymer chains has long been recognized as a basic prerequisite for biopolymer folding studies.[28,29] However, in marked contrast to the relatively mature studies of coil-to-globule transition thermodynamics, the relevant kinetic aspects have been far less experimentally explored, although a variety of theoretical models have been proposed.[30] Baysal and Karasz[30] have produced a comprehensive review article describing the whole situation.

Theoretical considerations of the kinetic problem of polymer collapse mainly employ three different approaches, including phenomenological models,[31–34] Langevin models,[35–44] and computer simulation studies.[43,45–54] According to the de Gennes model first proposed in 1985,[31] the collapsing chain can be viewed as a "sausage" of collapsed blobs with increasing thickness and decreasing length. Later on, Buguin and de Gennes et al.[32] revised the model and proposed that the transition into globules mainly proceed via two steps, namely the formation of "pearls" starting at the chain end and the subsequent coalescence of pearls into globules; they obtained a scaling of $\tau_{crum} \propto N^{1/2}$. Later on, Halperin et al.[34] proposed three-stage kinetics for the early stages of polymer collapse. The first step involves the formation of local clusters (pearls), the nascent droplets then grow by accreting monomers from the bridges that connect them (pearl necklace), and finally the droplets come into contact and coalesce into a single globule. The characteristic times of these three stages scale as N^0, $N^{1/5}$, and $N^{6/5}$, respectively. It should be noted that the early stage pearl necklace model has been inferred previously by Dawson et al.,[36,37,42] Pittard et al.[44] and Ostrovsky et al.[50] Compared to the model of Halperin,[34] the models proposed by Buguin et al.[32] and later by Klushin et al.[33] mainly deal with the collapsing kinetics of pearl necklaces. It should be noted that all the above described models do not consider topological constraints; the collapse of pearl necklace only leads to the formation of "crumpled globules" (τ_{crum}). As discussed by Grosberg et al.[55–58] and recently by Mansfield et al.,[57] internal segment entanglements (knotting) via slow reptation will dominate at later stages of chain collapse,[59] leading to the formation of final equilibrium globules (τ_{eq}).

To experimentally determine the coil-to-globule transition kinetics, an abrupt change of solvent quality is highly desired.[60] Previous experimentations in this field mainly employed the laser light scattering (LLS) technique.[61–69] The main limitation of the LLS facility in monitoring coil-to-globule transition kinetics is that quite a long (compared to chain collapsing time) thermal equilibration period is needed for temperature variation. Moreover, these experiments are typically conducted in the two phase region. Thus, the interference of interchain aggregation on monitoring the collapsing kinetics cannot be safely avoided.

The stopped-flow technique possesses a typical dead time of a few milliseconds and has been widely employed to investigate protein folding kinetics.[70] Recently, we employed a stopped-flow device coupled with a fluorescence detector to investigate the coil-to-globule transition kinetics of individual linear polymer chains in dilute solutions.[71] Using PNIPAM chains with a degree of polymerization (N) of 3 100, randomly labeled with pyrene moieties, we observed the two-stage coil-to-globule transition kinetics upon stopped-flow mixing extremely dilute polymer solution in methanol with an equal volume of water ($\varphi_{water} = 0.5$). To avoid possible interference from interchain aggregation, we only focused on the kinetics of the first few seconds after the jumping of solvent quality.[71] Two characteristic relaxation times, τ_{crum}, for the crumpling of a random coil (≈12 ms) and τ_{eq} for the relaxation from crumpled globule to compact globule (≈270 ms), were reliably obtained. The above experiments represent a deep quench depth since the solvent quality is jumping from good to deep below the coexistence curve (two-phase region), which is accompanied by the coil-to-compact globule transition.

It is noteworthy that a small and a large quench depth, ΔT, below the θ temperature lead to the formation of partially collapsed chains, i.e., crumpled globules and compact globules, respectively.[10,72] Frisch et al.[53] theoretically proposed that the relaxation pathway of the coil-to-globule transition strongly depends on the quench depth. A small value of ΔT below the θ temperature leads to isotropic chain collapse, whereas for relatively larger ΔT, the initial density fluctuations grow to form local clusters (pearling). At even larger ΔT, sausage-like structures, as predicted by de Gennes,[31] will form. However, the above arguments still lack support from direct experimental evidence.

Based on the re-entrant coil-to-globule-to-coil transition behavior of PNIPAM in a methanol/water mixture,[27] it is known that the addition of varying amounts of water into PNIPAM solution in methanol will result in different quench depths below the θ-solvent condition. Herein, we further investigate the coil-to-globule transition kinetics of PNIPAM chains upon jumping the solvent quality from pure methanol (good solvent, $\varphi_{water} = 0$) to methanol/water mixtures with varying φ_{water}. We focused on investigating the kinetics of chain contraction (from extended random coil to above the θ-state) and the random coil-to-crumpled globule transition. To avoid interference from the possible

Macromolecular Journals
DOI: 10.1002/macp.201000476

presence of interchain aggregation in the latter case (coil-to-crumpled globule transition), appropriate quench depths (jumping the solvent quality from good to the phase region below the θ-solvent condition and just around the coexistence curve), polymer concentration, and time windows of monitoring (only for the first few seconds) were screened.

Experimental Part

Materials

N-Isopropylacrylamide (NIPAM, 97%, Tokyo Kasei Kagyo Co.) was purified by recrystallization from a mixture of benzene and *n*-hexane (1/3, v/v). Acryloyl chloride was prepared by reacting acrylic acid with phosphorus trichloride. Azobisisobutyronitrile (AIBN) was recrystallized from 95% ethanol. 1-Pyrenebutanol was purchased from Aldrich. Other reagents were used as received. 4-(1-Pyrenyl)butyl acrylate (PyBA) was synthesized according to literature procedures.[73]

Sample Preparation

Synthesis of Pyrene-Labeled PNIPAM

Free radical copolymerization of NIPAM with PyBA in benzene at 55 °C using AIBN as the initiator led to PNIPAM samples randomly labeled with pyrene.[71] The resultant PNIPAM-*Py* copolymer was fractionated by successive dissolution/precipitation cycles at 30 °C in a mixture of extremely dried acetone and *n*-hexane. The third fraction denoted PNIPAM-*Py*-F_3 was selected for the current study. Size exclusion chromatography (SEC) analysis of PNIPAM-*Py*-F_3 in *N*,*N*-dimethylformamide in the presence of 1.0 g · L^{-1} LiBr at 60 °C revealed an $\overline{M}_n$ of 3.64 × 10^5 g · mol^{-1} and an $\overline{M}_w/\overline{M}_n$ of 1.17 (using polystyrene standards). The average molar ratio of NIPAM units to PyBA units for PNIPAM-*Py*-F_3 is ≈46, as determined using a method described previously.[71] On average, there are 65 pyrene groups per PNIPAM chain.

Characterization

Size Exclusion Chromatography (SEC)

Molecular weight distributions were determined by SEC using a series of three linear Styragel columns (HT3, HT4, and HT5) and an oven temperature of 60 °C. A Waters 1515 pump and a Waters 2414 differential refractive index detector (set at 30 °C) were used. The eluent was DMF + 1 g · L^{-1} LiBr at a flow rate of 1.0 mL · min^{-1}.

Laser Light Scattering (LLS)

A commercial spectrometer (ALV/DLS/SLS-5022F) equipped with a multi-tau digital time correlation (ALV5000) and a cylindrical 22 mW UNIPHASE He-Ne laser (λ_0 = 632 nm) as the light source was used for dynamic LLS measurements. Scattered light was collected at a fixed angle of 15° for a time period until the measured value was stable. Distribution averages and particle size distributions were computed using cumulants analysis and CONTIN routines. All data were averaged over three measurements. All LLS experiments were conducted at 25 ± 0.1 °C.

Fluorescence Measurements

Fluorescence spectra were recorded using a Shimazu RF-5301PC spectrofluorometer at a scan rate of 5 500 nm · min^{-1}. The temperature of the water-jacketed cell holder was controlled at 25 °C. The slit widths were set at 10 nm for excitation and 2.5 nm for emission. Polymer concentrations were fixed at 1 × 10^{-6} g · mL^{-1}.

Stopped-Flow Light Scattering and Fluorescence

Stopped-flow studies were carried out using a Bio-Logic SFM300/S stopped-flow instrument.[74–77] The SFM-300/S is a 3-syringe (10 mL) instrument in which all step-motor-driven syringes (S1, S2, S3) can be operated independently to carry out single or double mixing. The SFM-300/S stopped-flow device was attached to the MOS-250 spectrometer through an optical fiber connection. 30 shots were done successively for each mixing ratio and an average dynamic curve was obtained; kinetic data were fitted using the Biokine program (Bio-Logic). For the detection of light scattering intensity, both the excitation and emission wavelengths were adjusted to 335 nm, while for fluorescence detection, the excitation wavelength was set at 330 nm, and the emission wavelengths were respectively set at 378 nm and 480 nm to record the time-dependent intensity of monomer and excimer fluorescence. 5 nm slits were typically used for both the excitation and emission monochromator. Using an FC-08 or FC-15 flow cell, the typical dead times of the stopped-flow were about 1.1 ms and 2.6 ms, respectively. Temperature was maintained at 25 °C by circulating water around the syringe chamber and observation head.

The stopped-flow device is schematically illustrated in Scheme 1. An experiment using a basic stopped-flow apparatus is quite

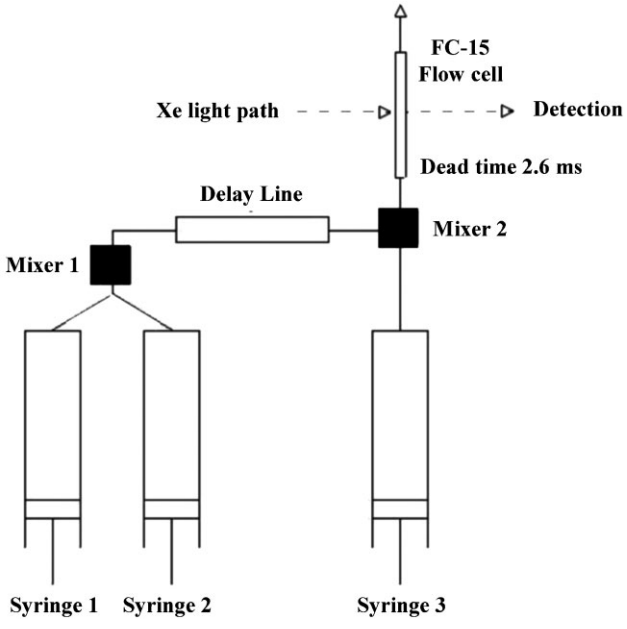

Scheme 1. Schematic illustration of the stopped-flow device and its liquid paths inside.

simple in principle.[70] The Bio-Logic SFM300 stopped-flow uses the drive motor to rapidly fire two solutions, contained in separate drive syringes driven by separate motors, together into a mixing device. The solutions then flow into the observation cell, displacing the previous contents with freshly mixed reactants. Motors cease to push at a given time to limit the volume of solution expended with each experiment and also serve to abruptly stop the flow. In addition, a hard stop was used to guarantee the quality of the stop. The fresh reactants in the observation cell are illuminated by a light source and the change, as a function of time, in many optical properties (absorbance, fluorescence, light scattering, turbidity, fluorescence anisotropy etc.) can be measured. The measurement of these optical properties is performed by the detectors, which can be mounted either perpendicular or parallel to the path of incoming light. Regardless of the stopped-flow configuration, the time resolution is limited by the time required for the reactants to flow from the final point of mixing to the observation cell. This time is referred to as the dead time of the instrument. The stop of the flow was dually controlled by the 3 separate motors and the hard-stop. Although the mixed solution is subjected to large shear forces before the stop, the effective light scattering detection starts 1 – 3 ms (the dead time) after the stop, thus we assume that shear forces before the stop will not result in any appreciable effects.

Results and Discussion

Phase Diagram of PNIPAM-*Py*-F_3 in Methanol/Water Mixture

An aqueous solution of PNIPAM exhibits unusual properties when it is triggered by temperature changes or the addition of water-miscible solvents, such as methanol.[12] Decreasing the temperature enhances its solubility and increasing the temperature induces macroscopic phase separation. PNIPAM in aqueous solution typically possesses a LCST of ≈32 °C. The addition of methanol into the aqueous solution can continuously shift the LCST from 32 to −5 °C when the volume fraction of water, φ_{water}, decreases from 1.0 to 0.45. Further decreasing φ_{water} leads to the abrupt increase of LCST.[24,25,78] At a fixed temperature of 25 °C and relatively high concentration (1×10^{-3} g · mL^{-1}), PNIPAM in a methanol/water mixture exhibits phase separation and the solution is cloudy in the φ_{water} range of 0.35 – 0.85.[24,25,78]

In extremely dilute solution, single chain collapse, i.e., a coil-to-globule transition, can be expected to occur since interchain aggregation will be greatly reduced. A typical phase diagram ($T \approx c$) of PS in cyclohexane shows the coexistence curve, below which phase separation will occur.[79,80] Sandwiched between the θ-region and the coexistence curve is the one-phase region, where single chain collapse can be observed.[72] In the current study, a pyrene-labeled PNIPAM sample was used. We needed to first elucidate the effects of introducing ≈2 mol-% of pyrene into PNIPAM on its phase diagram, and investigate the φ_{water} range, polymer concentrations, and suitable time window under which conditions for single chain collapsing kinetics could be monitored without any interference from interchain aggregation.

LCSTs are typically measured by turbidity and calorimetric scans,[24,25] but these techniques are only applicable for relatively high concentrations (≈1×10^{-3} g · mL^{-1}). At quite low concentrations (≈1×10^{-6} g · mL^{-1}), the solution may still appear clear and transparent, even if interchain aggregation occurs. Here we employed stopped-flow light scattering as a facile technique to investigate the φ_{water} range in which interchain aggregation will occur. It should be noted that the scattered intensity (I) is proportional to the square of the mass of (M) of scattering objects, i.e., $I \approx M^2$.

Figure 1 shows the typical time dependence of scattered intensity upon stopped-flow mixing PNIPAM-*Py*-F_3 solution in methanol with water, and the final φ_{water} is varied. A concentration of 1.0×10^{-5} g · mL^{-1}, which is too high for single chain collapsing studies,[27] was intentionally chosen for sensitive detection of the φ_{water} range of interchain aggregation. We can tell from Figure 1 that at $\varphi_{water} \leq 0.325$ and $\varphi_{water} \geq 0.9$, the scattered intensity remains as a straight line, indicating the absence of interchain aggregation. In the φ_{water} range from 0.35 to 0.875, the scattered intensity increases abruptly with time upon stopped-flow mixing, clearly indicating interchain aggregation. This

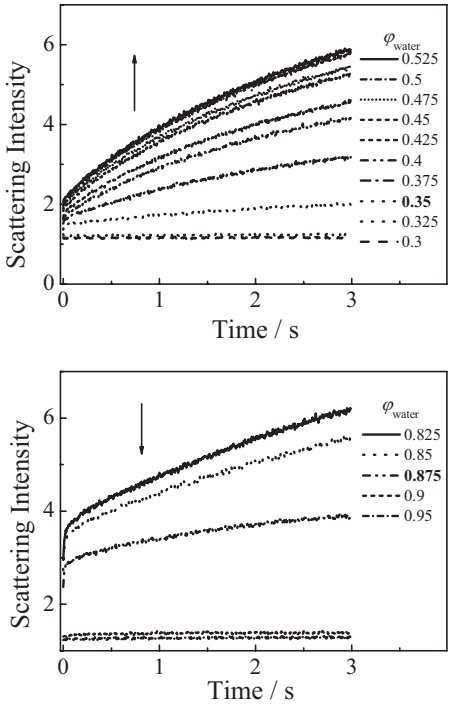

Figure 1. Time dependence of relative scattering intensity upon stopped-flow mixing of PNIPAM-*Py*-F_3 solution in methanol with varying amounts of water at 25 °C. The final polymer concentrations were fixed at 1.0×10^{-5} g · mL^{-1}. φ_{water} is the volume fraction of water in the mixed solvent.

Macromol. Chem. Phys. **2010**, *211*, 2573–2584

Macromolecular Journals

DOI: 10.1002/macp.201000476

φ_{water} range can be further categorized into two types, depending on the relative magnitudes of final scattering intensity values. In the φ_{water} range from 0.35 to 0.525, final scattering intensities increased with φ_{water}, whereas in the range from 0.825 to 0.875, the decrease of final scattering intensities with φ_{water} was observed. This agrees well with the chain collapsing behavior, i.e., re-entrant coil-to-globule-to-coil transition, of PNIPAM under highly dilute conditions, as previously reported by Wu and coworkers.[27] In the φ_{water} range from 0.35 to 0.525, an increasing extent of chain collapse and aggregation occurred, whereas in the φ_{water} range from 0.825 to 0.875, collapsed and aggregated chains underwent re-swelling. At $\varphi_{water} \geq 0.9$, no chain aggregation could even be observed.

For unlabeled PNIPAM homopolymer, its LCST was $\leq$25 °C in the φ_{water} range from 0.35 to 0.85.[24,25,78] Thus, these critical φ_{water} values obtained for PNIPAM-*Py*-F_3 agree fairly well with those of unlabeled PNIPAM. This confirms that the incorporation of $\approx$2 mol-% of pyrene moieties along the chain does not significantly affect the solution properties of PNIPAM. Relevant reports by Martinho et al.[19,21,81,82] and Winnik[83] also revealed that the incorporation of $\approx 1-5$ mol-% of pyrene units into PNIPAM chains does not result in discernible effects on their phase behavior.

We further employed LLS to determine the phase diagram and experimental conditions under which chain contraction (from extended coil to θ-state) and random coil-to-crumpled globule transition could be reliably observed without interference from interchain aggregation. To ensure enough detection sensitivity and accuracy, all LLS experiments were conducted at a final polymer concentration of 5.0×10^{-5} g · mL^{-1} considering that PNIPAM-*Py*-F_3 possesses an $\overline{M}_n$ of 3.64×10^5 g · mol^{-1}, which is much lower than that employed by Wu and co-workers for equilibrium collapsing transitions of PNIPAM chains ($\overline{M}_w \approx 2.6 \times 10^7$ g · mol^{-1}).[27] Figure 2 shows the variation of intensity-average hydrodynamic radius, $\langle R_h \rangle$, and scattering intensity as a function of φ_{water}. It was found that in the φ_{water} range from 0 to 0.28, $\langle R_h \rangle$ slightly decreased from 21.1 to 20.0 nm. In the range of φ_{water} from 0.28 to 0.325, $\langle R_h \rangle$ exhibited a more prominent decrease; $\langle R_h \rangle$ is 16.2 nm at $\varphi_{water} = 0.325$. At $\varphi_{water} > 0.325$, $\langle R_h \rangle$ abruptly increased, clearing indicating the occurrence of interchain aggregation at a polymer concentration of 5.0×10^{-5} g · mL^{-1} (Figure 2a).

In combination with the φ_{water}-dependent scattering intensity (Figure 2b), we can conclude that PNIPAM-*Py*-F_3 chains are in the one-phase region at $\varphi_{water} \leq 0.325$. Moreover, the θ-solvent condition for the aqueous solution of PNIPAM-*Py*-F_3 at 25 °C can be estimated to be $\varphi_{water} \approx 0.28$ from the plot of $\langle R_h \rangle$ vs solvent composition, according to protocols previously proposed by Wu.[84] In the φ_{water} range from 0 to 0.28, chain contraction occurs as the solvent quality gradually worsens, which is accompanied with the transition from the extended random coil conformation to the unperturbed conformation at the θ-solvent condition, whereas upon jumping from $\varphi_{water} = 0$ to the final φ_{water} range from 0.28 to 0.325, the random coil-to-crumpled globule transition in the one phase region can be observed.[27]

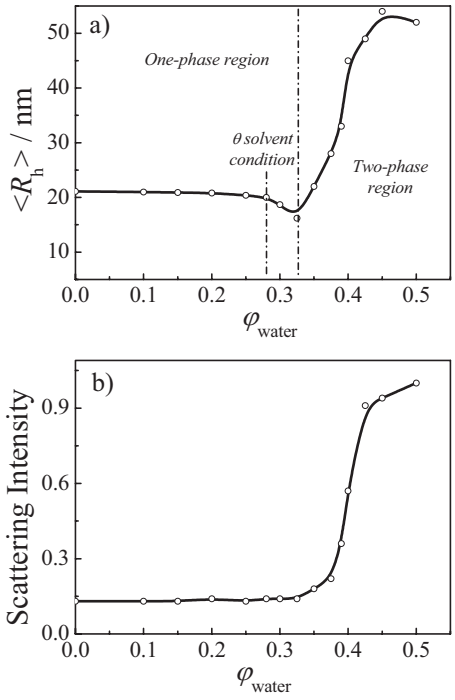

Figure 2. Variation of (a) intensity-average hydrodynamic radius, $\langle R_h \rangle$, and (b) normalized scattering intensity obtained for PNIPAM-*Py*-F_3 in methanol/water mixtures as a function of the volume fraction of water, φ_{water}. Dynamic LLS measurements were conducted at a scattering angle of 15° and polymer concentrations were fixed at 5.0×10^{-5} g · mL^{-1}.

It should be noted that, in subsequent kinetic experiments, the final polymer concentrations were fixed at 1.0×10^{-6} g · mL^{-1}, thus the one-phase region determined at a concentration of 5.0×10^{-5} g · mL^{-1} (Figure 2a) can ensure that chain collapsing kinetic studies in the final φ_{water} range of 0.28 to 0.325 fall into the phase region below the θ-solvent condition and above the coexistence curve. Actually, the competition between single chain collapse and interchain aggregation is highly polymer concentration dependent. Figure 3 shows the time dependence of the scattering intensity for PNIPAM-*Py*-F_3 at different final concentrations and a fixed φ_{water} of 0.45, at which prominent interchain aggregation can be observed by stopped-flow light scattering and LLS at a concentration of 1.0×10^{-5} and 5.0×10^{-5} g · mL^{-1}, respectively (Figure 1 and 2). When the final polymer concentration is higher than 2.0×10^{-6} g · mL^{-1}, we could observe the increase of scattered intensity with time, whereas scattered intensity

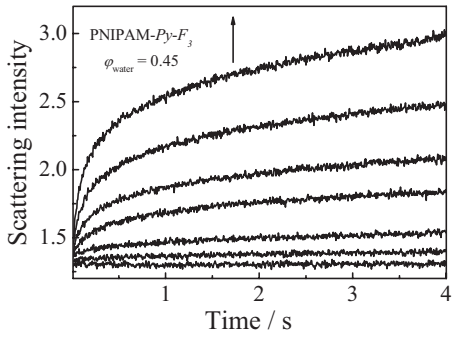

Figure 3. Time dependence of relative scattering intensity upon stopped-flow mixing PNIPAM-*Py*-F_3 solution in methanol with water at 25 °C, where final φ_{water} was fixed at 0.45. From top to bottom, final PNIPAM-*Py*-F_3 concentrations were 2.5×10^{-5}, 2.0×10^{-5}, 1.5×10^{-5}, 1.0×10^{-5}, 5.0×10^{-6}, 2.0×10^{-6}, and 1.0×10^{-6} g · mL^{-1}, respectively.

remained a straight line at least for the first 4 s with time when the polymer concentration was 1.0×10^{-6} g · mL^{-1}. Figure 4 shows the variation of scattering intensity with time upon stopped-flow jump from $\varphi_{water} = 0$ to final φ_{water} in the range 0.1 – 0.9. In all cases, all kinetic curves remained as straight lines, further verifying that no apparent interchain aggregation could be discerned for the first 4 s at a final polymer concentration of 1.0×10^{-6} g · mL^{-1} (Figure 4).

Fluorescence Studies of PNIPAM-*Py*-F_3 in Methanol/Water Mixture

It is well-known that pyrene forms a cofacial excimer when two pyrene molecules are close (<4 Å) and excited by a light of ≈330 nm.[85] Pyrene excimers exhibit characteristic fluorescence emission, which is distinct from isolated pyrene molecules. The excimer is stable only in its excited state and is affected by the collision with adjacent pyrene molecules. Excimer fluorescence of pyrene reports on the ability of two pyrene molecules coming into contact. For pyrene-labeled polymer chains, the latter is determined by the chain mobility and local pyrene concentrations.[86,87]

Martinho and Duhamel et al.[19,21,81,82] employed equilibrium excimer fluorescence to investigate the coil-to-globule transition thermodynamics of individual chains and a blob model was proposed accordingly.[86,87] The fluorescence technique enabled them to study the equilibrium collapsing transitions of short chains when labeled with appropriate fluorescent dyes. The high sensitivity of fluorescence also allowed the use of very dilute solutions. For pyrene-labeled PS ($\overline{M}_w = 1.13 \times 10^4$ g · mol^{-1}) in cyclohexane, they monitored the temperature dependence of the excimer-to-monomer fluorescence intensity ratio, I_e/I_m. It was found that I_e/I_m decreased upon decreasing the temperature from 60 to 10 °C, exhibiting an inflection point at ≈25 °C. The inflection temperature was ascribed to the θ-temperature. Decreasing the temperature to <10 °C led to apparent interchain aggregation, and I_e/I_m considerably increased.[21]

The fluorescence spectra of PNIPAM-*Py*-F_3 at different methanol/water mixtures are shown in Figure 5, where the final polymer concentrations were fixed at 1×10^{-6} g · mL^{-1}. From discussions in the previous section, we know that, even at such a low concentration, slight interchain aggregation will occur at extended time periods

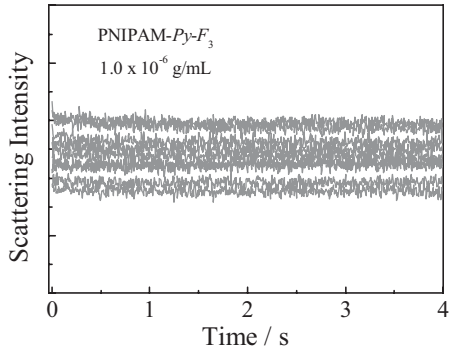

Figure 4. Time dependence of scattering intensity upon stopped-flow mixing of PNIPAM-*Py*- F_3 solution in methanol with different amounts of water at 25 °C. The final polymer concentrations were fixed at 1.0×10^{-6} g · mL^{-1}, respectively. φ_{water} values range from 0.1 to 0.9 and the interval between each line is 0.1.

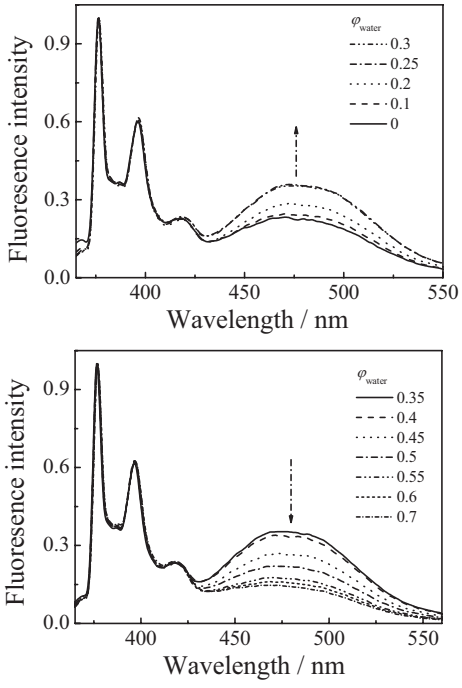

Figure 5. Emission fluorescence spectra recorded on a Shimazu RF-5301PC spectrofluorometer for PNIPAM-*Py*-F_3 in methanol/water mixture at different φ_{water}. The final PNIPAM-*Py*-F_3 concentration was fixed at 1.0×10^{-6} g · mL^{-1}.

Macromol. Chem. Phys. **2010**, *211*, 2573–2584

Macromolecular Journals

DOI: 10.1002/macp.201000476

(typically > 1 min) in the range $0.35 \leq \varphi_{water} \leq 0.875$. In the fluorescence experiments, the spectra were collected ≈10 s after mixing the polymer solution in methanol with water in a couvette to eliminate the interference of possible interchain aggregation.

PNIPAM-*Py*-F_3 exists as individual extended random coils in pure methanol, and it is quite expected that its fluorescence spectrum will show an emission related to locally excited pyrene chromophores (intensity I_m, "monomer emission") with the [0,0] band located at 378 nm and a broad structureless peak centered at 480 nm due to the excimer emission (intensity I_e) (Figure 5). In methanol, identical excitation spectra were obtained for the emission monitored at 378 and 480 nm, and 480 nm, and I_e/I_m remained constant over a wide concentration range of 2×10^{-7}–2.5×10^{-5} g · mL^{-1}. This indicates that, in methanol, pyrene molecules only form intrachain excimers due to the dynamic encounter of an excited state with a ground state pyrene molecule.[85]

Pyrene has a water solubility of $\approx 1 \times 10^{-6}$ M, whereas it is highly soluble in methanol ($>1 \times 10^{-2}$ M). The high solubility of pyrene in methanol explains the absence of pyrene association for PNIPAM-*Py*-F_3 in pure methanol. For PNIPAM-*Py*-F_3 in water, I_e/I_m is ≈1.6 at a concentration of 1×10^{-6} g · mL^{-1}, which is quite high. This suggests that pyrene is highly hydrophobic and that extensive intra- and possibly inter-molecular hydrophobic associations exist in pure water. At the beginning, we were concerned that pyrenes would first quickly associate with each other upon the solvent jump from pure methanol to a methanol/water mixture,[71] followed by the collapsing of polymer chains. If that was the case, this would severely interfere with our observation of single chain collapsing kinetics.

The following experiments were conducted to elucidate this issue before we attempted a further step. Firstly, pyrene solubility in methanol/water was determined to be $\approx 1 \times 10^{-4}$ M at $\varphi_{water} = 0.5$, which was much higher than that in pure water. Secondly, I_e/I_m dramatically decreased from 1.6 to 0.22 upon addition of ≈10 v/v% methanol into the aqueous solution of PNIPAM-*Py*-F_3; on the other hand, the I_e/I_m value is 0.23 for PNIPAM-*Py*-F_3 in pure methanol. At $\varphi_{water} = 0.9$, we varied the polymer concentration from 2×10^{-7} to 2.5×10^{-5} g · mL^{-1}, it was found that I_e/I_m did not change with polymer concentrations. Moreover, identical excitation spectra were obtained for the emission monitored at 378 and 480 nm.[83] The absence of a hydrophobic association between pyrene groups in methanol/water with φ_{water} up to 0.9 is possibly due to the preferential association of methanol molecules to the polymer chain, which has been confirmed by electronic paramagnetic resonance (EPR) spectrometry studies of spin-labeled PNIPAM.[25] Finally, poly(*N,N*-dimethylacrylamide) (PDMA) does not exhibit co-non-solvency behavior in a methanol/water mixture,[88] and preliminary experiments revealed that pyrene-labeled PDMA (with a comparable ≈2 mol-% pyrene content) also did not exhibit any hydrophobic association in a methanol/water mixture at $\varphi_{water} \leq 0.9$.

From the above analysis, we excluded the possibility that hydrophobic associations between pyrene groups would occur in the methanol/water mixture at $\varphi_{water} \leq 0.9$. In the current investigation of chain collapsing kinetics, the final φ_{water} after mixing is in the range of 0 – 0.375, so we could safely exclude the possibility of preferential hydrophobic association between pyrene groups upon jumping the solvent composition from pure methanol to methanol/water mixtures in this φ_{water} range.

Figure 6 shows the variation of I_e/I_m as a function of φ_{water} at a polymer concentration of 1.0×10^{-6} g · mL^{-1}. At $\varphi_{water} \leq 0.325$, PNIPAM-*Py*-$F_3$ was in the one phase region (Figure 2a). On the other hand, in the two phase region ($0.35 \leq \varphi_{water} \leq 0.875$), interchain aggregation was typically observed ≈60 s after solvent jumps. In the range $0 \leq \varphi_{water} \leq 0.275$, I_e/I_m increased from 0.23 to 0.36. It should be noted that the θ-solvent condition at 25 °C was at $\varphi_{water} \approx 0.28$ (Figure 2a).[27,84] Thus, the solvent range $0 \leq \varphi_{water} \leq 0.275$ is above the θ-solvent condition. I_e/I_m values were determined by the mobility of chain segments and the relative spatial distances between neighboring pyrene groups.[21] The increase of I_e/I_m actually reflects the contraction of coil size. As the coil size gets smaller, relative spatial distances between pyrene groups decrease, enhancing the chances that neighboring pyrene groups will encounter each other.[85] Moreover, the decrease of repulsion interactions between chain segments will also increase the encounter possibility between neighboring pyrene groups. Winnik[83] previously investigated the temperature dependence of I_e/I_m for pyrene-labeled PNIPAM in water. They found that, below the LCST, I_e/I_m also increased with temperature, reaching a maximum at ≈29 °C; above this, I_e/I_m decreased with temperatures.

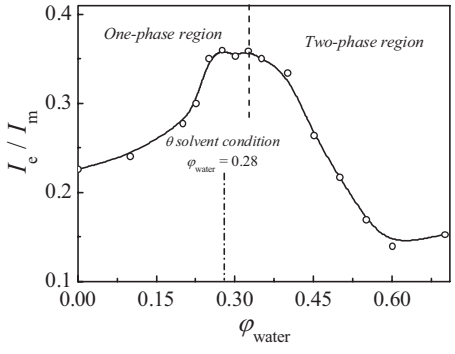

Figure 6. The excimer to monomer emission intensity ratios (I_e/I_m) obtained immediately after mixing PNIPAM-*Py*-F_3 solution in methanol with different amounts of water as a function of final φ_{water} at 25 °C. The final PNIPAM-*Py*-F_3 concentration was fixed at 1.0×10^{-6} g · mL^{-1}.

I_e/I_m exhibited a local plateau in the range $0.275 \leq \varphi_{water} \leq 0.325$. Above that, it continuously decreased up to $\varphi_{water} = 0.6$ and this clearly reflects the collapse of pyrene-labeled PNIPAM chains. The decrease of I_e/I_m reflects the decrease in chain mobility, hindering the rotation and diffusion of pyrene molecules on the chain so that pyrene molecules in the excited and ground state have less chance to encounter each other and form excimers. This is also in agreement with the excimer fluorescence results for pyrene-labeled PNIPAM reported by Winnik.[83] Note that Martinho et al.[19,21,81,89] also typically observed the decrease of I_e/I_m during equilibrium coil-to-globule transitions.

Kinetics of Chain Contraction and Random Coil-to-Crumpled Globule Transition

The previous two sections established the suitable range of solvent composition and polymer concentration for the monitoring of single chain contraction and collapsing kinetics. We then investigated the kinetics by monitoring the time dependence of I_e/I_m after stopped-flow mixing the polymer solution in methanol with different amounts of water. The final polymer concentration chosen was fixed at 1.0×10^{-6} g · mL^{-1}. The following discussion is thus divided into three sections, dealing with the chain contraction and collapsing kinetics under two circumstances: (1) upon jumping from pure methanol to the final range of $0 < \varphi_{water} \leq 0.275$, where the final solvent quality was above the θ-solvent condition, and polymer chains will partially contract due to the gradual worsening of solvent quality; (2) upon jumping from pure methanol to the range $0.28 \leq \varphi_{water} \leq 0.375$, where the solvent quality is below the θ-solvent condition and the exerted relatively small quench depth only leads polymer chains to partially collapse into crumpled globules.[27] Most importantly, polymer chains still exist in the one-phase region upon random coil-to-crumpled globule transition in the final range $0.28 \leq \varphi_{water} \leq 0.325$ (see Figure 2a). For the final range $0.325 < \varphi_{water} \leq 0.375$, which is just below the coexistence curve, we established from Figure 2–4 in previous sections that, at a final polymer concentration of 1.0×10^{-6} g · mL^{-1}, no apparent chain aggregation could be observed for the few 4 s upon stopped-flow jumping of solvent quality.

Stopped-Flow Jump from Good to Above the θ-Solvent Condition ($0 < \varphi_{water} \leq 0.275$)

Upon jumping the solvent condition from pure methanol to the range $0 < \varphi_{water} < 0.275$, the time dependence of I_e/I_m is shown in Figure 7a. At $\varphi_{water} \leq 0.175$, I_e/I_m remained a flat line, indicating that no apparent chain conformational changes could be discerned. We observed a small increase in the final equilibrium I_e/I_m values. This is qualitatively in agreement with the results shown in Figure 6, in which I_e/I_m increased in this range. It should be noted that a comparison of the absolute I_e/I_m values between those measured from a sophisticated spectrofluorometer (Figure 5 and 6) and those from the stopped-flow device (Figure 7) is meaningless, due to differences in apparatus set-up, sensitivity, and excitation/emission slits.

At $\varphi_{water} = 0.2$, 0.225, and 0.25, we could discern a small gradual decrease of I_e/I_m with time (Figure 7a), which stabilized out after ≈2 s. However, the decrease in I_e/I_m

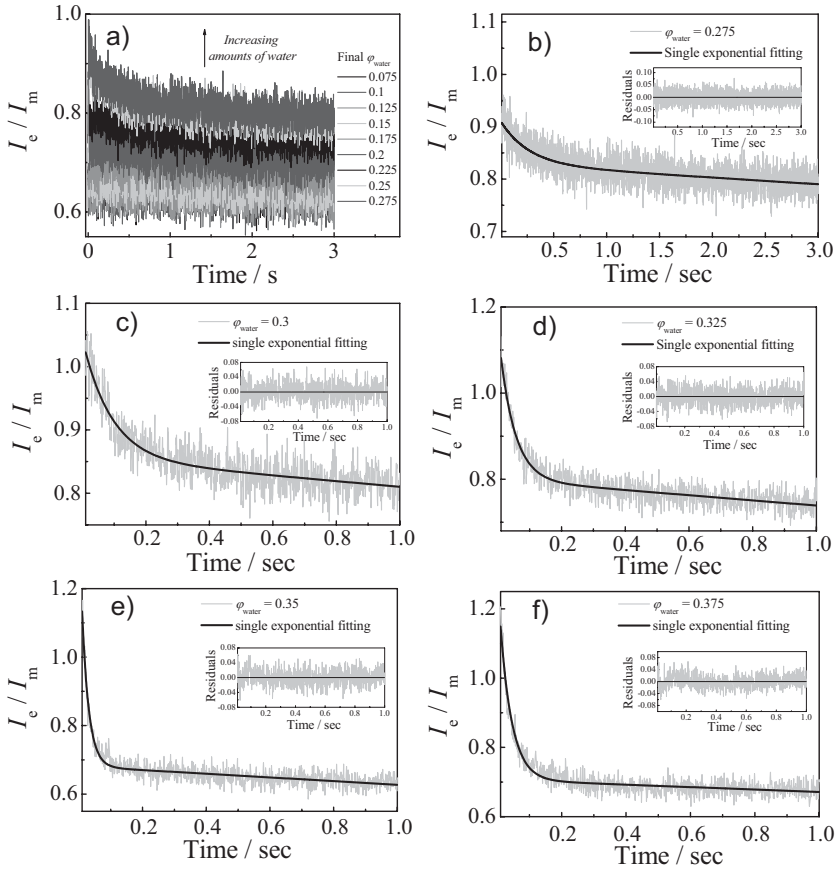

Figure 7. Time dependence of excimer to monomer emission intensity ratios (I_e/I_m) upon stopped-flow mixing PNIPAM-*Py*-F_3 solution in methanol with water. The final φ_{water} varied in the range 0.075 – 0.375 and the final polymer concentration was fixed at 1.0×10^{-6} g · mL^{-1}. Also shown are the single exponential fitting curves and fitting residuals.

Macromol. Chem. Phys. **2010**, *211*, 2573–2584

Macromolecular Journals

DOI: 10.1002/macp.201000476

with time is quite perplexing. We need to bear in mind that what we observed from stopped-flow fluorescence is the quick conformational changes of polymer chains in the mixed solvent. Actually it is ≈2.6 ms (stopped-flow dead time) after the fast and homogeneous mixing in mixer 2 (Scheme 1). Following a quick jump from pure methanol to $\varphi_{water} = 0.2$, 0.225, and 0.25, at which the solvent quality approaches further towards the θ-solvent condition, the coil size will slightly contract compared to that in pure methanol due to smaller repulsive chain segment-segment interactions; concomitantly, chain mobility also considerably decreases due to the worsening of solvent quality, leading to the decrease in I_e/I_m. We speculate here that the observed decrease of I_e/I_m with time in chain contraction kinetics can be ascribed to the mobility decrease of chain segments.

Single exponential fitting of dynamic traces obtained upon stopped-flow jumping to $\varphi_{water} = 0.2$, 0.225, and 0.25 led to characteristic relaxation times of 1.2 s, 0.64 s, and 0.27 s, respectively (Figure 7a and Figure 8). The relatively long characteristic times associated with coil contraction upon jumping the solvent quality from good to just above the θ-solvent condition should follow the Rouse-Zimm scaling,[90] i.e., $\tau_R \propto N^2$, which has been well-documented theoretically.[30–32,34] However, to the best of our knowledge, the current experiment represents the first direct example of obtaining the characteristic relaxation times of chain contraction kinetics upon solvent jumps from good to above the θ-solvent condition. Further work towards experimentally obtaining relevant scaling relationships is highly desirable to verify the above observations.

Random Coil-to-Crumpled Globule Transition Kinetics in the One-Phase Region ($0.28 \leq \varphi_{water} \leq 0.325$)

In this region, the final solvent quality is just below the θ-solvent condition and above the coexistence curve (Figure 1–2), but it can only be considered as a small quench depth apart from the θ-solvent. Only crumpled globules will form eventually.[27] Most importantly, we can clearly tell from Figure 1–2 that the kinetics of the coil-to-crumpled globule transition upon the jump from pure methanol to this solvent range can be obtained in the absence of any interchain aggregation, as polymer chains still locate in the one-phase region. From Figure 7, we can observe a more dramatic decrease of I_e/I_m with time upon jumping from pure methanol to the range $0.28 \leq \varphi_{water} \leq 0.325$, compared to those obtained for the final range of $0 < \varphi_{water} \leq 0.275$. The presence of a θ-solvent state at $\varphi_{water} = 0.28$ is clearly evident; above this critical φ_{water} value, chain collapse leads to more prominent time-dependent I_e/I_m decreases.

For comparison, we also integrated kinetic data at final φ_{water} values of 0.35 and 0.375 into Figure 7. It is worth noting that at $\varphi_{water} = 0.35$ and 0.375, PNIPAM-*Py*-F_3 chains are in the two-phase region; however, interchain aggregation for at least the first 4 s is negligible (Figure 3–4). The time dependence of I_e/I_m (defined as I_t) can be converted to a normalized function; namely, $(I_t - I_\infty)/I_\infty$ vs t, where I_∞ is I_t after an infinitely long time. It was found that all the dynamic curves in the range $0.30 \leq \varphi_{water} \leq 0.375$ could be fitted well with single exponential functions (Figure 7b–e):

$$(I_t - I_\infty)/I_\infty = ce^{-t/\tau} \quad (1)$$

where c is the normalized amplitude and τ is the characteristic relaxation time of the collapsing process from random coils to crumpled globules. A rough look at Figure 7a to 7f reveals that, in the final solvent range of $0.30 \leq \varphi_{water} \leq 0.375$, the coil-to-crumpled globule transition gets faster as φ_{water} increases. Figure 8 summarizes the final φ_{water} dependence of the characteristic relaxation time, τ. We can clearly tell that τ decreases continuously with φ_{water}, indicating a faster coil-to-crumpled globule transition.

The above analysis leads to the conclusion that, under a small quench depth below the θ-solvent condition, the coil-to-crumpled globule transition is a one-stage process, which is in agreement with the predication proposed by Frisch et al.[53] They proposed that a small value of ΔT below the θ temperature only leads to the isotropic one-stage collapse of polymer chains. However, as commented by Halperin et al.,[34] previous theoretical considerations proposed by Buguin and de Gennes et al.[32] and later by Frisch et al.[53] mainly focused on the collapsing kinetics of the pearl necklace and did not consider earlier events such as pearling and bridge stretching.

Extensive theoretical considerations over the past two decades concerning the coil-to-globule transition have led to a general consensus.[31–59] The collapsing scenario for flexible chains consists of the following sequences upon solvent jumps to below the θ condition: (1) fast pearling and bridge stretching leads to the formation of a "pearl

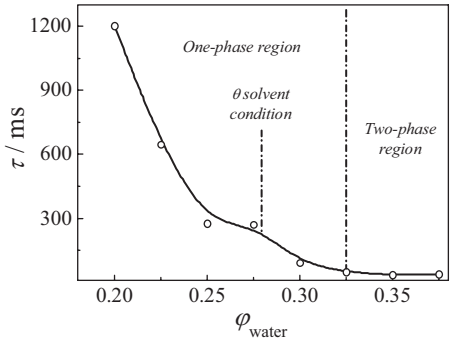

Figure 8. Quench depth dependence of characteristic relaxation times obtained from single exponential fitting of the dynamic curves shown in Figure 7. φ_{water} was in the range 0.2 – 0.375. Note that single exponential fitting of dynamic curves obtained at $\varphi_{water} < 0.2$ led to meaningless results.

necklace''; (2) coarsening stage (collapse of pearl necklace) and subsequent slow shape optimization leading to the formation of crumpled globules; (3) the final relaxation into compact globules via chain knotting and self-reptation.

As discussed by Halperin et al.,[34] the pearling and bridge stretching processes at the early stages of chain collapse are very fast (and might be on the order of microseconds[91]), as the characteristic relaxation time of pearling, τ_p, is independent of chain length (N^0). Considering that the stopped-flow device has a resolution of milliseconds, it was quite expected that we would not be able to observe the early pearling and bridge stretching processes. Upon jumping from pure methanol to the range $0.30 \leq \varphi_{water} \leq 0.325$, the observed one-stage collapsing kinetics in the one-phase region can be ascribed well to the collapse of pearl necklaces. It is worthy of noting that, under these experimental conditions, the quench depth is not large enough and the final state is crumpled globules.

On the other hand, we propose that the fast pearling and bridging processes, i.e., the formation of pearl necklaces, might be inferred from time-dependent I_e/I_m changes. From Figure 7c to 7f, we can discern that I_e/I_m values at $t = 0$ (i.e., 2.6 ms after solvent jumps) are relatively high as compared to the equilibrium I_e/I_m values for solvent mixtures in the range $0 < \varphi_{water} \leq 0.25$, which is above the θ-solvent condition; it then decreases with time and finally stabilizes out. The early stage (fast pearling and bridge stretching processes) can lead to the formation of local clusters embedded with a few neighboring pyrene molecules; moreover, at this stage chain segments can still move freely. This explains the high I_e/I_m value at $t = 0$ due to closer proximity of probe molecules. The subsequent collapse of pearl necklaces is accompanied with a decrease in segmental mobility, leading to decreasing I_e/I_m values with time.

Previous theoretical considerations of single chain collapsing kinetics indicated that during the formation of pearl necklaces, the coil size $\langle R_g \rangle^2$ decreases by a power law with collapsing time t. In the subsequent steps, i.e., the collapse of pearl necklaces and shape optimization, $\langle R_g \rangle^2$ exhibits a complex and an exponential decay with time, respectively.[30–32,34] For simplicity, the time-dependent I_e/I_m changes obtained in the current study were treated exponentially. Furthermore, the validity of this type of treatment can be argued as follows. (1) In protein folding kinetic studies, the exponential fitting of time-dependent fluorescence (intrinsic fluorescence of tryptophan residues, added ANS probes, FRET) changes has been typically employed, and the results generally agree with the time-dependence size changes.[92] (2) In a series of reports by Martinho et al.[19,21,81,82] and Duhamel et al.,[86,87,93] a blob model was proposed for the investigation of polymer chain folding by the fluorescence technique and successfully correlated the temperature dependence of I_e/I_m of pyrene-labeled chains with their size shrinkage during collapse. (3) It would be excellent to directly follow the time dependence of coil sizes during collapsing. We believe that a combination of stopped-flow with small angle X-ray scattering (SAXS) or small angle neutron scattering (SANS) may work; however, as an extremely dilute solution needs to be used to avoid interchain aggregation, this would be a severe technological challenge for the SAXS or SANS facility. As proposed by Halperin et al.,[34] the pearling and bridge stretching process might probably lead to no size changes at all. So even if directly monitoring the time-dependent size changes is possible, the early stage events will still be missing. (4) Considering the current availability of facilities, we believe that the combination of stopped-flow with fluorescence detection provides a suitable route to probe the chain contraction and collapsing kinetics in the early stages.

From Figure 8, we can tell that, in the range $0.30 \leq \varphi_{water} \leq 0.325$, the random coil-to-crumpled globule transition gets faster with increasing φ_{water}, i.e., increasing quenching depths. This is in marked contrast to de Gennes's original sausage model,[31] which predicted slower relaxation kinetics at larger quench depths. However, it agrees quite well with his revised model.[32] For the collapse of pearl necklaces, Halperin et al. proposed that $\tau \propto (N^{6/5}/g_c)\tau_\xi$, where N is the degree of polymerization of the chain, g_c is the number of monomers per collapse blob, and $\tau_\xi \propto (\theta/\Delta T)^2$. This predicts that $\tau \propto 1/\Delta T^2$, where ΔT can be viewed as the quench depths. Thus, τ will exponentially decreases with increasing ΔT, i.e., quench depth.

It should be noted that in Figure 8 relaxation times obtained from kinetic traces upon the stopped-flow jump from pure methanol to the φ_{water} range of 0.2–0.375 are all plotted. Across the θ-solvent condition at $\varphi_{water} = 0.28$, no dramatic variation of τ with φ_{water} can be discerned. This is reasonable considering that the θ-condition is actually a manually assigned ideal state, in which chains exhibit nearly unperturbed dimensions because chain segment-segment interactions just balance the chain segment-solvent interactions. It seems that the collapse of pearl necklaces will not recognize the θ-condition, i.e., chain contraction and chain collapse kinetics upon jumping the solvent quality from good to above and just below the θ-condition, respectively, might not differ dramatically. A continuous coil-to-crumpled globule transition is thus implied.[94–96] Furthermore, although pyrene-labeled PNIPAM chains are in the two phase region at $\varphi_{water} = 0.35$ and 0.375, the stopped-flow kinetic study within the first 4 s is safe to exclude the interference from interchain aggregation (Figure 3–4), as evidenced by the smooth variation of τ across the coexistence curve, i.e., there is no appreciable changes of τ at φ_{water} values >0.325 or <0.325.

In combination with our previous report concerning the chain collapsing kinetics in the deep quench region ($\varphi_{water} = 0.5$),[71] we conclude that the quench depths can

Macromol. Chem. Phys. 2010, 211, 2573–2584
Macromolecular Journals
DOI: 10.1002/macp.201000476

exhibit dramatic effects on the collapsing pathways and the corresponding characteristic relaxation times. At small quench depths from good to just below the θ-solvent condition, the coil-to-crumpled globule transition is an isotropic one-stage process. At deeper quench depths ($\varphi_{water} > 0.4$), the final state is compact globules,[27] and the coil-to-compact globule transition is at least a two-stage process, revealing two characteristic relaxation times.[71]

Conclusion

In summary, chain contraction and random coil-to-crumpled globule transition kinetics of pyrene-labeled flexible PNIPAM chains ($\overline{M}_n = 3.64 \times 10^5\ g \cdot mol^{-1}$, $\overline{M}_w/\overline{M}_n = 1.17$) were systematically investigated via a combination of stopped-flow fluorescence and light scattering techniques upon jumping the solvent composition from pure methanol to varying methanol/water mixtures. The effects of quench depths on the single chain collapsing pathways and characteristic relaxation times were obtained. We have focused on investigating the kinetics of chain contraction (from extended random coil to above the θ-state) and the random coil-to-crumpled globule transition upon jumping the solvent quality from good to the phase region below the θ-solvent condition and just around the coexistence curve.

The introduction of ≈2 mol-% pyrene units into PNIPAM chains resulted in negligible effects on its phase behavior in methanol/water mixtures. At $\varphi_{water} \leq 0.9$, intra- or intermolecular hydrophobic associations between hydrophobic pyrene labels did not occur, possibly due to the preferential association of methanol molecules to the polymer chain. The possibility of fast initial hydrophobic associations between pyrene groups upon solvent jumps can be successfully excluded.

We successfully established that the quench depths can exhibit dramatic effects on the collapsing pathways. At small quench depths below the θ-solvent condition, the coil-to-crumpled globule transition is an isotropic one-stage process. At deeper quench depths, the final state is compact globule, and the coil-to-compact globule transition is at least a two-stage process.[71]

Acknowledgements: Financial support from the *National Natural Scientific Foundation of China (NNSFC)* Projects 20674079, 20874092, and 51033005 and the *Specialized Research Fund for the Doctoral Program of Higher Education (SRFDP)* is gratefully acknowledged.

Received: August 10, 2010; Revised: September 1, 2010; Published online: October 21, 2010; DOI: 10.1002/macp.201000476

Keywords: chain; fluorescence; light scattering; mixing; phase behavior

[1] P. J. Flory, *Principles of Polymer Chemistry*, Cornell University Press, Ithaca, New York 1952.
[2] I. M. Lifshitz, A. Y. Grosberg, A. R. Khokhlov, *Rev. Mod. Phys.* **1978**, *50*, 683.
[3] G. Allegra, F. Ganazzoli, F. Bignotti, M. Bolognesi, *Biopolymers* **1990**, *29*, 1823.
[4] V. S. Pande, A. Y. Grosberg, T. Tanaka, *Folding and Design* **1997**, *2*, 109.
[5] M. Sadqi, L. J. Lapidus, V. Munoz, *Proc. Natl. Acad. Sci. USA* **2003**, *100*, 12117.
[6] W. H. Stockmayer, *Makromol. Chem.* **1960**, *35*, 54.
[7] S. T. Sun, I. Nishio, G. Swislow, T. Tanaka, *J. Chem. Phys.* **1980**, *73*, 5971.
[8] G. Swislow, S. T. Sun, I. Nishio, T. Tanaka, *Phys. Rev. Lett.* **1980**, *44*, 796.
[9] M. Meewes, J. Ricka, M. Desilva, R. Nyffenegger, T. Binkert, *Macromolecules* **1991**, *24*, 5811.
[10] M. A. Moore, *J. Phys. A: Math. Gen.* **1977**, *10*, 305.
[11] A. Y. Grosberg, D. V. Kuznetsov, *Macromolecules.* **1992**, *25*, 1980.
[12] H. G. Schild, *Prog. Polym. Sci.* **1992**, *17*, 163.
[13] C. Wu, S. Q. Zhou, *Macromolecules* **1995**, *28*, 8381.
[14] C. Wu, S. Q. Zhou, *Macromolecules* **1995**, *28*, 5388.
[15] S. Q. Zhou, S. Y. Fan, S. C. F. Auyeung, C. Wu, *Polymer* **1995**, *36*, 1341.
[16] B. M. Baysal, N. Kayaman, *J. Chem. Phys.* **1998**, *109*, 8701.
[17] C. Wu, X. H. Wang, *Phys. Rev. Lett.* **1998**, *80*, 4092.
[18] N. Kayaman, E. E. Gurel, B. M. Baysal, F. E. Karasz, *Polymer* **2000**, *41*, 1461.
[19] S. Picarra, P. Relogio, C. A. M. Afonso, J. M. G. Martinho, J. P. S. Farinha, *Macromolecules* **2003**, *36*, 8119.
[20] Y. Maki, N. Sasaki, M. Nakata, *Macromolecules* **2004**, *37*, 5703.
[21] S. Picarra, J. Duhamel, A. Fedorov, J. M. G. Martinho, *J. Phys. Chem. B* **2004**, *108*, 12009.
[22] C. Wu, S. Q. Zhou, *Phys. Rev. Lett.* **1996**, *77*, 3053.
[23] N. Yoshinaga, D. J. Bicout, E. I. Kats, A. Halperin, *Macromolecules* **2007**, *40*, 2201.
[24] H. G. Schild, M. Muthukumar, D. A. Tirrell, *Macromolecules* **1991**, *24*, 948.
[25] F. M. Winnik, M. F. Ottaviani, S. H. Bossmann, M. Garciagaribay, N. J. Turro, *Macromolecules* **1992**, *25*, 6007.
[26] F. M. Winnik, M. F. Ottaviani, S. H. Bossmann, W. S. Pan, M. Garciagaribay, N. J. Turro, *Macromolecules* **1993**, *26*, 4577.
[27] G. Z. Zhang, C. Wu, *J. Am. Chem. Soc.* **2001**, *123*, 1376.
[28] S. E. Jackson, *Folding and Design* **1998**, *3*, R81.
[29] L. L. Qiu, C. Zachariah, S. J. Hagen, *Phys. Rev. Lett.* **2003**, *90*, 168103.
[30] B. M. Baysal, F. E. Karasz, *Macromol. Theory Simul.* **2003**, *12*, 627.
[31] P. G. de Gennes, *J. Phys. Lett.* **1985**, *46*, L639.
[32] A. Buguin, F. Brochard Wyart, P. G. deGennes, *C. R. Acad. Sci. Paris, Ser. II, B* **1996**, *322*, 741.
[33] L. I. Klushin, *J. Chem. Phys.* **1998**, *108*, 7917.
[34] A. Halperin, P. M. Goldbart, *Phys. Rev. E* **2000**, *61*, 565.
[35] F. Ganazzoli, R. Laferla, G. Allegra, *Macromolecules* **1995**, *28*, 5285.
[36] E. G. Timoshenko, K. A. Dawson, *Phys. Rev. E* **1995**, *51*, 492.

[37] E. G. Timoshenko, Y. A. Kuznetsov, K. A. Dawson, *J. Chem. Phys.* **1995**, *102*, 1816.
[38] N. Yoshinaga, K. Yoshikawa, T. Ohta, *Eur. Phys. J. E* **2005**, *17*, 485.
[39] E. Pitard, *Eur. Phys. J. B* **1999**, *7*, 665.
[40] E. Pitard, H. Orland, *Europhys. Lett.* **1998**, *41*, 467.
[41] Y. A. Kuznetsov, E. G. Timoshenko, K. A. Dawson, *J. Chem. Phys.* **1996**, *105*, 7116.
[42] Y. A. Kuznetsov, E. G. Timoshenko, K. A. Dawson, *J. Chem. Phys.* **1996**, *104*, 3338.
[43] Y. A. Kuznetsov, E. G. Timoshenko, K. A. Dawson, *J. Chem. Phys.* **1995**, *103*, 4807.
[44] T. Garel, H. Orland, E. Pittard, *Spin Glasses and Random Fields*, World Scientific, Singapore 1998.
[45] G. Tanaka, W. L. Mattice, *Macromol. Theory Simul.* **1996**, *5*, 499.
[46] A. Byrne, P. Kiernan, D. Green, K. A. Dawson, *J. Chem. Phys.* **1995**, *102*, 573.
[47] G. Tanaka, W. L. Mattice, *Macromolecules* **1995**, *28*, 1049.
[48] M. Wittkop, S. Kreitmeier, D. Goritz, *Computational and Theoretical Polymer Science* **1996**, *6*, 41.
[49] A. Milchev, K. Binder, *Europhys. Lett.* **1994**, *26*, 671.
[50] B. Ostrovsky, Y. Bar-Yam, *Europhys. Lett.* **1994**, *25*, 409.
[51] B. Schnurr, F. Gittes, F. C. MacKintosh, *Phys. Rev. E* **2002**, *65*, 061904.
[52] M. P. Taylor, *J. Chem. Phys.* **2001**, *114*, 6472.
[53] T. Frisch, A. Verga, *Phys. Rev. E* **2002**, *66*, 041807.
[54] S. H. Lee, R. Kapral, *J. Chem. Phys.* **2006**, *124*, 124901.
[55] A. Y. Grosberg, D. V. Kuznetsov, *Macromolecules* **1993**, *26*, 4249.
[56] A. Y. Grosberg, S. K. Nechaev, E. I. Shakhnovich, *J. Phys. France* **1988**, *49*, 2095.
[57] M. L. Mansfield, *J. Chem. Phys.* **2007**, *127*, 244902.
[58] Y. Rabin, A. Y. Grosberg, T. Tanaka, *Europhys. Lett.* **1995**, *32*, 505.
[59] A. L. Kholodenko, T. A. Vilgis, *Phys. Rep. -Rev. Sec. Phys. Lett.* **1998**, *298*, 254.
[60] P. V. Yushmanov, I. Furo, I. Iliopoulos, *Macromol. Chem. Phys.* **2006**, *207*, 1972.
[61] B. Chu, Q. C. Ying, A. Y. Grosberg, *Macromolecules* **1995**, *28*, 180.
[62] B. Chu, Q. C. Ying, *Macromolecules* **1996**, *29*, 1824.
[63] J. Q. Yu, Z. L. Wang, B. Chu, *Macromolecules* **1992**, *25*, 1618.
[64] N. Kayaman, E. E. Gurel, B. M. Baysal, F. E. Karasz, *Macromolecules* **1999**, *32*, 8399.
[65] M. Nakata, Y. Nakamura, Y. Maki, N. Sasaki, *Macromolecules* **2004**, *37*, 4917.
[66] Y. Nakamura, N. Sasaki, M. Nakata, *Macromolecules* **2001**, *34*, 5992.
[67] M. Nakata, T. Nakagawa, *J. Chem. Phys.* **1999**, *110*, 2703.
[68] M. Nakata, Y. Nakamura, N. Sasaki, *Phys. Rev. E* **2007**, *76*, 041805.
[69] Y. Maki, T. Dobashi, M. Nakata, *J. Chem. Phys.* **2007**, *126*, 134901.
[70] K. A. Johnson, *Kinetic Analysis of Macromolecules: A Practical Approach*, Oxford University Press, New York 2003.
[71] J. Xu, Z. Y. Zhu, S. Z. Luo, C. Wu, S. Y. Liu, *Phys. Rev. Lett.* **2006**, *96*, 027802.
[72] C. Williams, F. Brochard, H. L. Frisch, *Ann. Rev. Phys. Chem.* **1981**, *32*, 433.
[73] J. Xu, S. Z. Luo, W. F. Shi, S. Y. Liu, *Langmuir* **2006**, *22*, 989.
[74] Z. Y. Zhu, S. P. Armes, S. Y. Liu, *Macromolecules* **2005**, *38*, 9803.
[75] S. Z. Luo, S. Y. Liu, J. Xu, H. Liu, Z. Y. Zhu, M. Jiang, C. Wu, *Macromolecules* **2006**, *39*, 4517.
[76] D. Wang, T. Wu, X. J. Wan, X. F. Wang, S. Y. Liu, *Langmuir* **2007**, *23*, 11866.
[77] D. Wang, J. Yin, Z. Y. Zhu, Z. S. Ge, H. W. Liu, S. P. Armes, S. Y. Liu, *Macromolecules* **2006**, *39*, 7378.
[78] R. O. R. Costa, R. F. S. Freitas, *Polymer* **2002**, *43*, 5879.
[79] M. Nakata, T. Dobashi, Y. Inakuma, K. Yamamura, *J. Chem. Phys.* **1999**, *111*, 6617.
[80] M. Nakata, T. Dobashi, N. Kuwahara, M. Kaneko, B. Chu, *Phys. Rev. A* **1978**, *18*, 2683.
[81] S. Picarra, P. T. Gomes, J. M. G. Martinho, *Macromolecules* **2000**, *33*, 3947.
[82] J. P. S. Farinha, S. Picarra, K. Miesel, J. M. G. Martinho, *J. Phys. Chem. B* **2001**, *105*, 10536.
[83] F. M. Winnik, *Macromolecules* **1990**, *23*, 233.
[84] C. Wu, M. Li, X. H. Wang, *Chin. J. Polym. Sci.* **1999**, *17*, 367.
[85] J. B. Briks, *Photophysics of Aromatic Molecules*, Wiley, New York 1970.
[86] J. Duhamel, *Acc. Chem. Res.* **2006**, *39*, 953.
[87] J. Duhamel, S. Kanagalingam, T. J. O'Brien, M. W. Ingratta, *J. Am. Chem. Soc.* **2003**, *125*, 12810.
[88] K. Pagonis, G. Bokias, *Polymer* **2004**, *45*, 2149.
[89] S. Picarra, J. M. G. Martinho, *Macromolecules* **2001**, *34*, 53.
[90] I. Teraoka, *Polymer Solutions: An Introduction to Physical Properties*, John Wiley & Sons, New York 2002.
[91] X. D. Ye, Y. J. Lu, L. Shen, Y. W. Ding, S. L. Liu, G. Z. Zhang, C. Wu, *Macromolecules* **2007**, *40*, 4750.
[92] C. A. Royer, *Chem. Rev.* **2006**, *106*, 1769.
[93] A. K. Mathew, H. Siu, J. Duhamel, *Macromolecules* **1999**, *32*, 7100.
[94] A. Y. Grosberg, A. R. Khokhlov, *Statistical Physics of Macromolecules*, AIP Press, New York 1994.
[95] H. Fujita, *Polymer Solutions*, Elsevier, New York 1990.
[96] J. J. Des Cloizeau, G. Jannink, *Polymers in Solution, their Modeling and Structure*, Oxford Science Publishers New York 1990.

Macromolecular Journals
DOI: 10.1002/macp.201000476